NON-RIGID MULTI-FRAME REGISTRATION OF LIVE CELL MICROSCOPY IMAGES

Marco Tektonidis, Il-Han Kim, and Karl Rohr

University of Heidelberg, BIOQUANT, IPMB, and DKFZ Heidelberg,
Dept. Bioinformatics and Functional Genomics, Biomedical Computer Vision Group,
Im Neuenheimer Feld 267, 69120 Heidelberg, Germany

ABSTRACT

Live cell microscopy images enable to study the motion of subcellular particles for understanding biological processes within cells. For accurate quantification of the particle motion, compensation of the motion and deformation of the cell nucleus is required. We introduce a multi-frame non-rigid registration approach for live cell microscopy image sequences. Compared to existing approaches using pairwise registration, our approach exploits information from multiple consecutive images simultaneously to improve the robustness and to enforce temporal consistency. Our approach has been successfully applied to live cell microscopy image sequences and an experimental comparison with pairwise registration has been carried out.

***Index Terms*—** Biomedical image processing, Image sequence analysis, Multi-frame registration

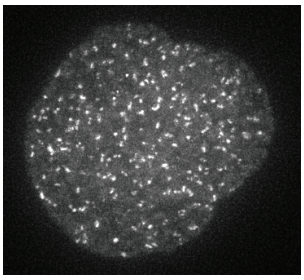
1. INTRODUCTION

Analyzing the time-resolved behavior of subcellular particles based on live cell microscopy images yields important information about the underlying biological processes. However, in the images both the motion and deformation of a cell as well as the motion of particles within the cell are observed (Fig. 1). Thus, a quantitative analysis of particle motion directly on the original image data is inaccurate since a superposition of the particle motion and the motion and deformation of the cell is obtained. To cope with this problem, the dynamic image sequences can be registered w.r.t. a certain reference time point. Registration approaches yield a mapping of physical points along the sequence of images, which can be used to compensate cell motion and deformation.

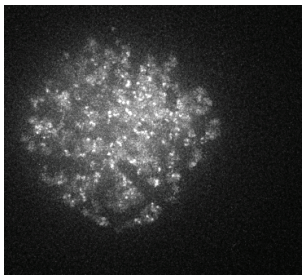
In previous work, different non-rigid registration approaches have been proposed to compensate cell motion and deformation in microscopy image data. Mattes et al. [1], for example, described a landmark-based registration approach for cell nuclei using thin-plate splines. Yang et al. [2] used an extension of the Demons algorithm based on symmetric forces to register images of different cells as well as live cell microscopy images. Kim et al. [3] introduced an extension of the Lucas-Kanade optic flow algorithm for the registration of dynamic cell nuclei images. A contour-based non-rigid registration method which utilizes thin-plate splines has been proposed by De Vylder et al. [4] for registration of cell nuclei. For 3D reconstruction of live cell microscopy images, Du et al. [5] introduced an intensity-based non-rigid registration approach using thin-plate splines.

All approaches described above for non-rigid registration of dynamic cell microscopy images employ *pairwise* temporal registration. In pairwise registration, each frame of a sequence is registered either to a chosen reference frame (*reference* registration method) or to the previous frame (*consecutive* registration method). For registration of cell nuclei the consecutive method is preferred, since it can cope better with intensity variations of cell nuclei over time. Pairwise registration decomposes the 2D+t or 3D+t registration task into multiple independent 2D or 3D registration tasks. Thus, the solution may be temporally inconsistent since the pairwise scheme is based solely on the information of two successive images. However, *temporal consistency* of a 2D+t or 3D+t transformation is advantageous since it ensures continuity of a physical point along the temporal dimension of an image sequence.

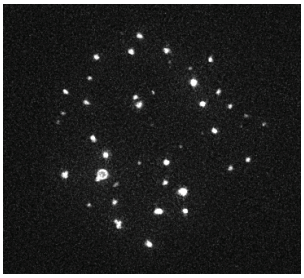
In this work, we propose a new intensity-based approach for non-rigid *multi-frame* registration of cell nuclei in time-lapse microscopy images. In our approach, each image of an image sequence is registered to the reference image at the first time point by exploiting information from multiple consecutive images and by taking into account computed transformations from previous time steps. Thus, compared to pairwise registration, we take advantage of additional temporal information to improve the robustness and we take into account transformations of previous time steps to enforce temporal consistency. Our multi-frame non-rigid registration approach has been applied to multi-channel microscopy images, i.e., the transformations are computed based on the first channel (nucleus channel) and are applied for registration of the second channel (particle channel). We have quantitatively evaluated our approach based on live cell microscopy image data and have performed an experimental comparison with a previous pairwise registration approach.



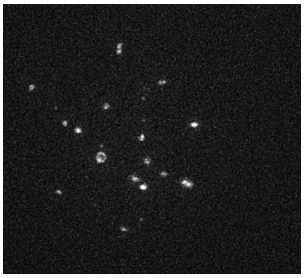
(a) Cell nucleus ($t = 0$)



(b) Cell nucleus ($t = 60$)



(c) Particles ($t = 0$)



(d) Particles ($t = 60$)

Fig. 1. Example images from a two-channel microscopy image sequence (contrast-enhanced). (a),(b) Cell nucleus in channel 1, (c),(d) Particles in channel 2.

2. METHODS

In this section, we first describe the general incremental scheme of our temporal registration approach. Then, we introduce our multi-frame consecutive non-rigid registration approach and describe the used iterative registration scheme. Finally, we formulate a multi-frame weighting approach based on optic flow estimation.

2.1. Incremental temporal registration scheme

Our approach is based on an incremental scheme, where each image g_k of an image sequence at time point $k \geq 2$ is registered to the reference image g_1 at the first time point. First, the transformation of the image g_k to the image g_{k-1} is computed and represented by a dense deformation vector field $\mathbf{u}(g_k, g_{k-1})$. Then, the transformation of g_k to g_1 is obtained by concatenating $\mathbf{u}(g_k, g_{k-1})$ and $\mathbf{u}(g_{k-1}, g_1)$:

$$\mathbf{u}(g_k, g_1) = G * \left(\mathbf{u}\left(g_k, g_{k-1}\right) \circ \mathbf{u}\left(g_{k-1}, g_1\right)\right), \qquad (1)$$

where $\mathbf{u}(g_{k-1}, g_1)$ is computed analogously (recursively), $\mathbf{u}(g_1, g_1)$ is a zero vector field, and G represents a Gaussian kernel for temporal regularization of the vector field.

2.2. Multi-frame consecutive non-rigid registration approach

In our approach, we estimate for each time point k the deformation vector field $\mathbf{u}(g_k, g_{k-1})$ by exploiting the information from $N \geq 3$ consecutive images of an image sequence simultaneously. The image g_k is registered simultaneously to the $N-1$ warped previous images, for which the transformations have been computed in previous time steps. Note however, that $N-1$ previous images are available only for $k \geq N$. Generally, for a time point k, the temporal range of available previous images g_l is given by $\max(k-N+1, 1) \leq l \leq k-1$, and the number of the available previous images is $N_l = \min(N-1, k-1)$.

Since the searched vector field $\mathbf{u}(g_k, g_{k-1})$ describes the transformation between the coordinate systems of g_k and g_{k-1}, the N_l previous images g_l have to be warped into the coordinate system of g_{k-1}. For warping, a vector field $\mathbf{u}(g_l, g_{k-1})$ is required, which can be determined by combining vector fields that have been computed for images at previous time points. For example, to determine $\mathbf{u}(g_{k-3}, g_{k-1})$ for warping of g_{k-3}, we concatenate the vector fields $\mathbf{u}(g_{k-2}, g_{k-3})$ and $\mathbf{u}(g_{k-1}, g_{k-2})$, and invert the resulting vector field. In general, each image g_l is warped using the following vector field:

$$\mathbf{u}(g_l, g_{k-1}) = G * \left[\mathbf{u}\left(g_{k-1}, g_l\right)\right]^{-1}, \qquad (2)$$

where $\mathbf{u}\left(g_{k-1}, g_l\right) = G * \left[\mathbf{u}\left(g_{l+1}, g_l\right) \circ \mathbf{u}\left(g_{k-1}, g_{l+1}\right)\right]$ is calculated recursively using computed vector fields of previous time points, and $\mathbf{u}\left(g_{k-1}, g_{k-1}\right)$ is a zero vector field. In (2) the inverse vector field is determined based on a weighted average of vectors that point closest to an image point. Our multi-frame consecutive registration approach minimizes for each time point k the sum of a similarity metric S between the image g_k and the images g_l:

$$\mathbf{u}(g_k, g_{k-1}) = \qquad (3)$$
$$\arg\min_{\mathbf{u}} \frac{1}{N_l} \sum_l S\left[g_k\left(\mathbf{T}\left(\mathbf{x}, \mathbf{u}\right)\right), g_l\left(\mathbf{T}\left(\mathbf{x}, \mathbf{u}(g_l, g_{k-1})\right)\right)\right]$$

where $\mathbf{T}\left(\mathbf{x}, \mathbf{u}\right)$ denotes the transformation using the vector field $\mathbf{u}$, $\mathbf{x}$ is the spatial coordinate, $g_k\left(\mathbf{T}\left(\mathbf{x}, \mathbf{u}\right)\right)$ is the image at time point k warped with $\mathbf{u}$, and $g_l\left(\mathbf{T}\left(\mathbf{x}, \mathbf{u}(g_l, g_{k-1})\right)\right)$ is the image at time point l warped using (2). A diagram of the multi-frame consecutive registration approach is shown in Fig. 2.

The optimal vector field $\mathbf{u}$ in (3) minimizes the sum of the similarity metric between the image g_k and each previous warped image at time point l. By using additional images compared to pairwise registration, we exploit additional information to increase the robustness, and by using vector fields computed for images at previous time points, we enforce temporal consistency of the registration result.

2.3. Iterative registration scheme

Our approach uses an iterative scheme which computes the searched vector field $\mathbf{u}(g_k, g_{k-1})$ at each iteration i by:

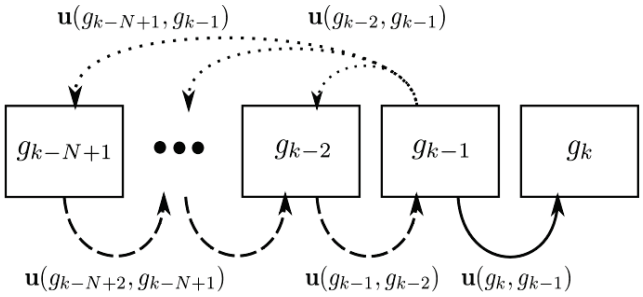


Fig. 2. Diagram of the multi-frame consecutive registration approach. The searched transformation $\mathbf{u}(g_k, g_{k-1})$ (solid arrow) is computed as follows: the image g_k is registered to the previous $N-1$ warped images. Warping is performed using transformations (dotted arrows), which have been obtained by registering images at previous time points (dashed arrows).

$$\mathbf{u}_i(g_k, g_{k-1}) = G * (\mathbf{u}_{i-1}(g_k, g_{k-1}) + G * d\mathbf{u}_i(g_k^*, g_{k-1})), \quad (4)$$

where $g_k^* = (\mathbf{T}(\mathbf{x}, \mathbf{u}_{i-1}(g_k, g_{k-1})))$ is the transformed image at time point k using the vector field from the previous iteration, and $d\mathbf{u}_i(g_k^*, g_{k-1})$ is an *update field*. The initial vector field $\mathbf{u}_0(g_k, g_{k-1})$ is the zero vector field. The iteration terminates either when a certain number of iterations is reached or when the sum of the similarity metric in (3) is below a certain threshold value.

2.4. Multi-frame weighting non-rigid registration approach

For the minimization problem (3), we integrate a *weighting* registration approach [3] based on optic flow estimation. The weighting approach has been previously used for pairwise registration of microscopy images and it performed better than other optic flow based registration approaches, e.g., symmetric Demons [2] and Lucas-Kanade [3, 6]. The *pairwise weighting* approach is based on the optimization method of Levenberg-Marquardt and minimizes for each image point the squared intensity differences between pairs of successive images.

Here, we extend this approach for application to multi-frame registration. The *multi-frame weighting* approach minimizes for each image point $\mathbf{x}_c$ the sum of squared intensity differences between the image g_k^* and the N_l previous warped images. The optimization is performed for each time point k over a spatial neighborhood region Ω around each pixel $\mathbf{x}_c$:

$$\min_{\mathbf{U}} \sum_{\mathbf{x}\in\Omega} \frac{1}{N_l} \sum_l \left[g_k^*(\mathbf{x}+\mathbf{U}) - g_l^\star(\mathbf{x})\right]^2, \quad (5)$$

where $g_l^\star(\mathbf{x}) = g_l(\mathbf{T}(\mathbf{x}, \mathbf{u}(g_l, g_{k-1})))$ denotes the warped image at time point l, and $\mathbf{U}$ is the vector of the update field $d\mathbf{u}_i(g_k^*, g_{k-1})$ at position $\mathbf{x}_c$. Note, that a *local* transformation model $\mathbf{x}+\mathbf{U}$ is used since the optimization is performed separately for each pixel $\mathbf{x}_c$. The sum of squared intensity differences in (5) corresponds to the similarity metric S in (3). Linearization of (5) yields:

$$\sum_{\mathbf{x}\in\Omega} \frac{1}{N_l} \sum_l \left(\nabla g_k^* \nabla g_k^{*T} + \mathbf{D}_{l,i}\right) \mathbf{U} = \sum_{\mathbf{x}\in\Omega} \frac{1}{N_l} \sum_l \nabla g_k^* \left(g_l^\star - g_k^*\right), \quad (6)$$

from which $\mathbf{U}$ can be determined. Note, that g_k^*, ∇g_k^*, and $g_l^\star$ are evaluated at $\mathbf{x}$. $\mathbf{D}_{l,i}$ is a diagonal matrix which indicates whether the current estimate of $\mathbf{U}$ is close to the solution. The elements of the matrix are given by $D_{l,nn} = c\, w_l(\mathbf{x}) \left(\partial g_k^*/\partial x_n\right)^2$, where c is a constant. The weighting function $w_l(\mathbf{x})$ is computed for each pixel $\mathbf{x}$ by:

$$w_l(\mathbf{x}) = \frac{\left(|\nabla g_l^\star| - |\nabla g_k^*|\right)^2}{2\left(|\nabla g_l^\star|^2 + |\nabla g_k^*|^2\right)} + \frac{\left|\arccos\left(\frac{\nabla g_l^\star \nabla g_k^*}{|\nabla g_l^\star||\nabla g_k^*|}\right)\right|}{2\pi}, \quad (7)$$

and quantifies the similarity between the image g_k^* and each image $g_l^\star$ on the basis of the image gradient magnitude (first term) and the gradient orientation (second term). For identical gradients, $w_l(\mathbf{x})$ is zero and for dissimilar gradients it is close to one.

3. EXPERIMENTAL RESULTS

We have applied our multi-frame non-rigid registration approach to real microscopy image data of live cells. We used four 2D fluorescence microscopy image sequences, which consist of 100 up to 200 images with a resolution of 384×384 up to 512×512 pixels (the data has kindly been provided by Y.-C. Chen and D.L. Spector, CSHL). The first channel displays nuclei of human cells, and the second channel displays subcellular particles (e.g., Fig. 1). Note, that the cells in these image sequences are going into mitosis and undergo strong deformations.

For a quantitative evaluation and a comparison with a previous pairwise approach we used manually tracked structures in the image sequences. For each sequence, positions of 9 spot-like structures within cell nuclei were tracked for 28 up to 83 subsequent time points. For each structure and each time point we computed the registration error as the Euclidean distance to the position of the structure at the first image. In all our experiments we used $\sigma = 2$ for the standard deviation of the Gaussian kernel for regularization of the vector fields.

For our multi-frame registration approach we used different numbers of frames ($N = 3, 5, 10, 20, 30, 50$) and compared the result to pairwise registration ($N = 2$). As an example, we show the registration error for a spot-like structure in an image sequence (Fig. 3). It can be seen, that the multi-frame approach (for all values of N) achieves a lower registration error than the pairwise approach (solid line). Multi-frame registration with $N = 3$ reduces the mean error e_{mean}

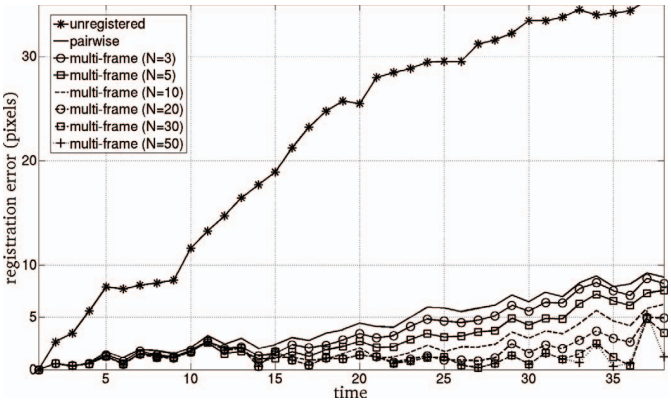


Fig. 3. Registration error for one tracked spot-like structure in a real image sequence as a function of time for multi-frame registration (for different values of $N \geq 3$) and pairwise registration ($N = 2$).

[pixels]	$\overline{e}_{mean}$					$\overline{e}_{max}$
	Sequence					
	A	B	C	D	Average	Average
unreg.	6.56	13.97	26.65	27.84	18.76	33.26
pairwise	3.23	2.87	4.39	7.08	4.39	9.61
multi-frame $N = 3$	3.03	2.76	3.82	6.40	$4.00_{-9\%}$	$9.08_{-6\%}$
multi-frame $N = 5$	3.04	2.52	3.63	5.68	$3.72_{-15\%}$	$8.96_{-7\%}$
multi-frame $N = 10$	2.84	2.33	3.45	4.64	$3.31_{-25\%}$	$\mathbf{8.4_{-13\%}}$
multi-frame $N = 20$	2.73	2.21	**3.31**	4.10	$\mathbf{3.09_{-30\%}}$	$9.07_{-6\%}$
multi-frame $N = 30$	2.67	**2.14**	3.89	4.03	$3.18_{-28\%}$	$9.95_{+4\%}$
multi-frame $N = 50$	**2.57**	2.53	4.06	**3.97**	$3.28_{-25\%}$	$10.5_{+9\%}$

Table 1. Registration error for 9 tracked spot-like structures for four real image sequences using multi-frame and pairwise registration. Percentages indicate the change compared to pairwise registration.

by 15%, and for $N = 10$ and $N = 30$ the improvement is 50% and 72%, respectively. The averaged mean error $\overline{e}_{mean}$ over all 9 spot-like structures for each of the four image sequences A,B,C,D is shown in Table 1. It can be seen, that the multi-frame approach with $N = 3$ yields better results than the pairwise approach, and the result is further improved by increasing N up to a certain value of N. If we average $\overline{e}_{mean}$ over all four image sequences, the best result is obtained for $N = 20$ (see the column "Average"), achieving a reduction of the registration error of 30% compared to the pairwise approach.

To study the reliability of the registration results in terms of outliers we also determined the maximum error e_{max} for each spot-like structure. The averaged maximum error $\overline{e}_{max}$ over all structures of all four image sequences is also shown in Table 1 (right column). Compared to pairwise registration, multi-frame registration with $N = 3$ reduces $\overline{e}_{max}$ by 6%, and the best result is obtained for $N = 10$ with an improvement of 13%. For $N \geq 20$, $\overline{e}_{max}$ is increasing and for $N \geq 30$, $\overline{e}_{max}$ is larger than for pairwise registration, which is an indication of outliers due to the very different intensity structure of the nuclei within the relatively large temporal range. The optimal number of frames N for multi-frame registration should be chosen based on the application, i.e. whether $\overline{e}_{mean}$ or $\overline{e}_{max}$ is more important. For our application, considering both $\overline{e}_{mean}$ and $\overline{e}_{max}$, the optimal number of frames is $N = 10$ or $N = 20$.

4. DISCUSSION

We have presented a multi-frame intensity-based approach for non-rigid registration of cell microscopy image sequences. By exploiting multiple images simultaneously and taking into account transformations computed for previous time points, the robustness is increased and temporal consistency is enforced. Experimental results using live cell microscopy image data demonstrated an improvement of our approach compared to a previous pairwise registration approach.

Acknowledgements Support of the BMBF projects VIROQUANT (FORSYS) and EpiSys (SysTec) is gratefully acknowledged. This work benefited from the use of ITK.

5. REFERENCES

[1] J. Mattes, J. Nawroth, P. Boukamp, R. Eils, and K.M. Greulich-Bode, "Analyzing motion and deformation of the cell nucleus for studying co-localizations of nuclear structures," in *Proc. IEEE International Symposium on Biomedical Imaging: From Nano to Macro 2006 (ISBI'06)*, Arlington/VA, USA, 2006, pp. 1044 –1047.

[2] S. Yang, D. Köhler, K. Teller, T. Cremer, P. Le Baccon, E. Heard, R. Eils, and K. Rohr, "Nonrigid registration of 3-D multichannel microscopy images of cell nuclei," *IEEE Trans. on Image Processing*, vol. 17, no. 4, pp. 493–499, 2008.

[3] I.-H. Kim, Y.-C. Chen, D. Spector, R. Eils, and K. Rohr, "Non-rigid registration of 2D and 3D dynamic cell nuclei images for improved classification of subcellular particle motion," *IEEE Trans. on Image Processing*, vol. 20, no. 4, pp. 1011–1022, 2011.

[4] J. De Vylder, W. H. De Vos, E. M. Manders, and W. Philips, "2D mapping of strongly deformable cell nuclei, based on contour matching," *Cytometry Part A*, vol. 79A, no. 7, pp. 580–588, 2011.

[5] T. Du and M. Wasser, "3D image stack reconstruction in live cell microscopy of drosophila muscles and its validation," *Cytometry Part A*, vol. 75A, no. 4, pp. 329–343, 2009.

[6] J. L. Barron, D. J. Fleet, and S. S. Beauchemin, "Performance of optical flow techniques," *International Journal of Computer Vision*, vol. 12, no. 1, pp. 43–77, 1994.